Introduction to Medical Image Processing (5XSA0), Module 07

Part 01 Introduction to X-ray imaging

Peter H.N. de With

(p.h.n.de.with@tue.nl)

With Contributions from D. Ruijters of Philips Healthcare

slides version 1.0

Overview Module 07 Part 1 X-ray

- **Part 1a: Basic principles of X-ray**
  - EM radiation
  - X-ray tube and detection
- **Part 1b: Clinical techniques and applications**
  - Fused visualization
  - Registration in various types: rigid, elastic, vascular
  - Clinical applications:
    - (1) Needle registration and navigation during live interventions, and
    - (2) Stenting with live artery overlay visualization

An X-ray system: Philips X-ray C-arm

Basic principles: EM radiation – (1)

- **EM Radiation, examples**
  - Visible light, radio waves, x-rays, gamma rays
  - Has no mass, is unaffected my magnetic/electric fields,
  - constant speed through a medium (max. 3x10^8 m/s in vacuum)
  - Characterized by: photon wavelength, frequency, energy/ph E

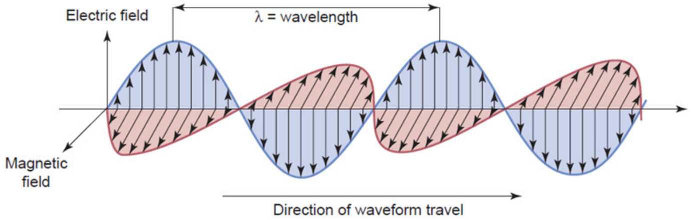

FIGURE 2-4 Electric and magnetic field components of EM radiation.

Basic principles: EM radiation – (2)

- **Photon energy**
  - Expressed in electron Volts (eV), typical medical MeV and keV
  - 1 eV is the energy to transfer the electron across 1 V difference potential in vacuum
- **Ionizing radiation**
  - Occurs when photons are in the far UV range of the spectrum
  - Wavelength lamba > 200 nm
  - Photon: sufficient energy to remove electrons from atomic shells leading to ionized atoms and molecules (for X-rays and gamma)
  - Ionizing state depends on the matter, ionizing energies for Calcium, glucose, liquid water are 6.1, 8.8 and 12.1 eV For the human body it is approx. 11 eV.

Basic principles: characteristic X-rays – (1)

- **Electron transitions: emission of radiation**
  - Spectrum can be in the range of visible, UV or X-ray
  - Large emissions > 100 eV give charact. or fluorescent X-rays
  - $E_{\text{x-ray}} = E_{\text{b vacant shell}} - E_{\text{b transition shell}}$ where b refer to binding an example is : M to K shell transition in Tungsten would produce a K-shell X-ray of 67 eV.
- **Gamma rays**
  - Radioactive decay often results in a daughter nucleus in an excited state
  - The EM radiation emitted when the nucleus goes to a lower but more stable state is gamma radiation

Basic principles: characteristic X-rays – (2)

- Example: Tungsten electron transition

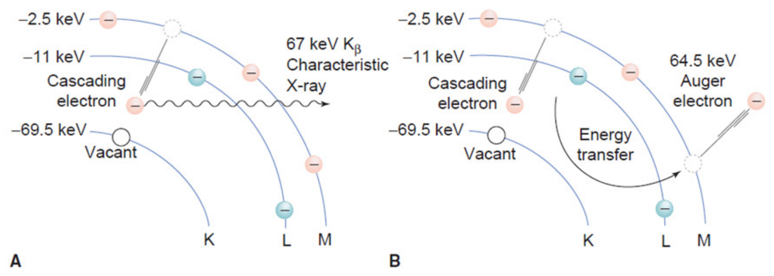

■ FIGURE 2-7 De-excitation of a tungsten atom. An electron transition filling a vacancy in an orbit closer to the nucleus will be accompanied by either the emission of characteristic radiation (**A**) or the emission of an Auger electron (**B**).

Basic principles: production of X-ray – (1)

- The X-ray tube with Tungsten material

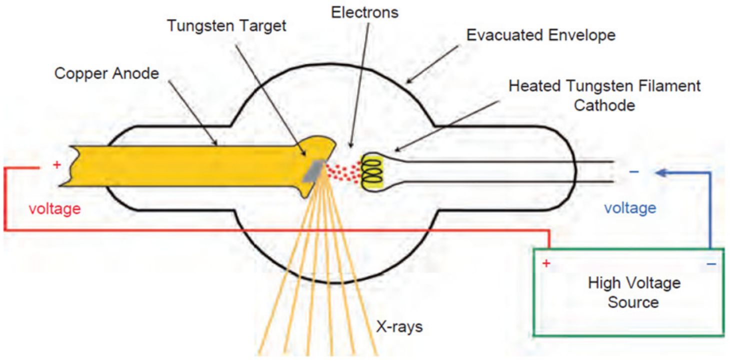

■ FIGURE 6-1 Minimum requirements for x-ray production include a source and target of electrons, an evacuated envelope, and connection of the electrodes to a high-voltage source.

Basic principles: production of X-ray – (2)

- **Different forms of radiation**

  Bremsstrahlung occurs when electrons interact with nucleus, loss of kinetic energy gives X-ray
- amount is inversely proportional to the interaction distance
- Only high-energy radiation is kept after filtering

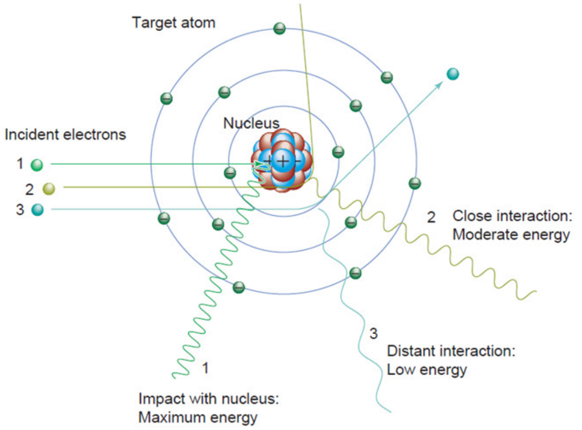

FIGURE 6-2 Bremsstrahlung radiation arises from energetic electron interactions with an atomic nucleus of the target material. In a "close" approach, the positive nucleus attracts the negative electron, causing deceleration and redirection, resulting in a loss of kinetic energy that is converted to an x-ray. The x-ray energy depends on the interaction distance between the electron and the nucleus; it decreases as the distance increases.

Basic principles: production of X-ray – (3)

- **X-ray tube example construction: principle**

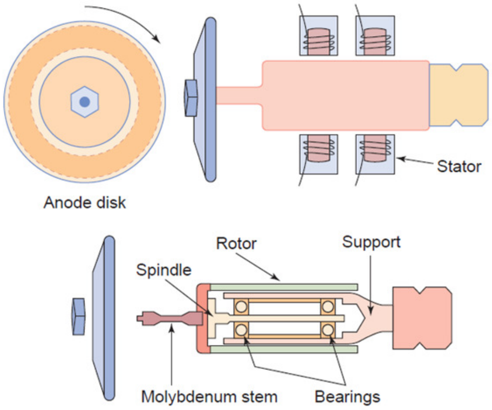

FIGURE 6-12 The anode of a rotating anode x-ray tube is a tungsten disk mounted on a bearing-supported rotor assembly (front view, **top left**; side view, **top right**). The rotor consists of a copper and iron laminated core and forms part of an induction motor. The other component is the stator, which exists outside of the insert, **top right**. A molybdenum stem (molybdenum is a poor heat conductor) connects the rotor to the anode to reduce heat transfer to the rotor bearings (**bottom**).

Basic principles: production of X-ray – (4)

- X-ray tube example construction: focal spot length

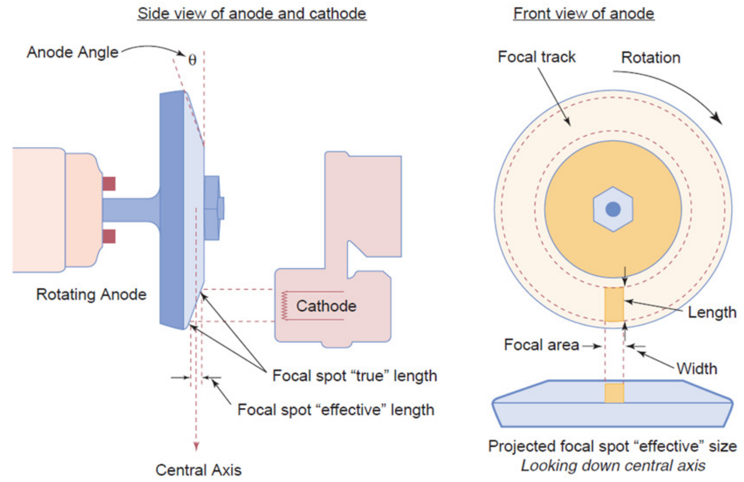

■ **FIGURE 6-13** The anode (target) angle, θ, is defined as the angle of the target surface in relation to the central ray. The focal spot length, as projected down the central axis, is foreshortened, according to the line focus principle (**lower right**).

Basic principles: production of X-ray – (5)

- **Focal length**
  - Effective focal spot length is smaller due to geometry projection
  - Effective focal length = actual focal length x sin(theta)

EXAMPLE 1: The actual anode focal area for a 20-degree anode angle is 4 mm (length) by 1.2 mm (width). What is the projected focal spot size at the central axis position?

Answer: Effective length = actual length × sin θ = 4 mm × sin 20 degrees = 4 mm × 0.34 = 1.36 mm; therefore, the projected focal spot size is 1.36 mm (length) by 1.2 mm (width).

EXAMPLE 2: If the anode angle in Example 1 is reduced to 10 degrees and the actual focal spot size remains the same, what is the projected focal spot size at the central axis position?

Answer: Effective length = 4 mm × sin 10 degrees = 4 mm × 0.174 = 0.69 mm; thus, the smaller anode angle results in a projected size of 0.69 mm (length) by 1.2 mm (width) for the same actual target area.

Basic principles: production of X-ray – (6)

- Shaping the radiation beam with collimator blades

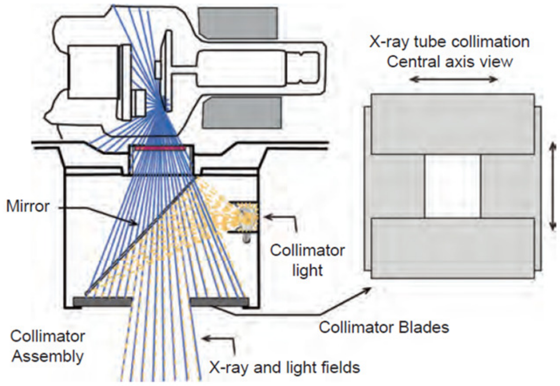

FIGURE 6-19 The x-ray tube collimator assembly is attached to the housing at the tube port, typically on a collar that allows it to be rotated. A light source, positioned at a virtual focal spot location, illuminates the field from a 45-degree angle mirror. Lead collimator blades define both the x-ray and light fields.

X-ray attenuation through the human

$$I = I_0\, e^{-\int \mu(x)dx}$$

- I and I_0 are output and input X-ray intensities
- μ is the attenuation along the ray path

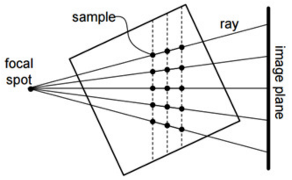

Ruijters et al.: "GPU-Accelerated Digitally Reconstructed Radiographs", Proc. BioMed, 2008, pp 431-435

Basic principles: Detection of X-ray – (1)

- **Detection with CCD chip**
  - Time-delay and integration system (TDI)
  - CCD chip is read-out at a velocity –V
  - Synchronizing read-out with scanning motion above patient, the signal at detection travels through entire field of view of detector (addressing all dexels = detection elem'ts)

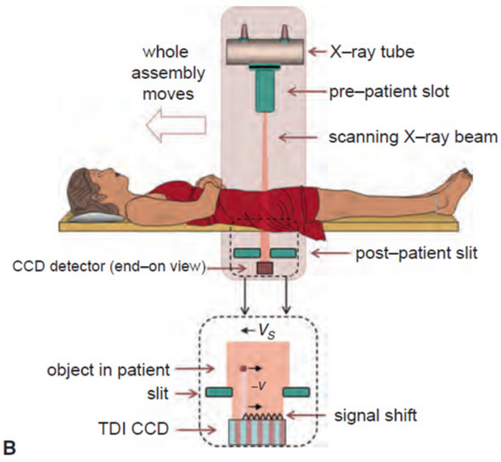

Basic principles: Detection of X-ray – (2)

- **Detection w. TFT panels**

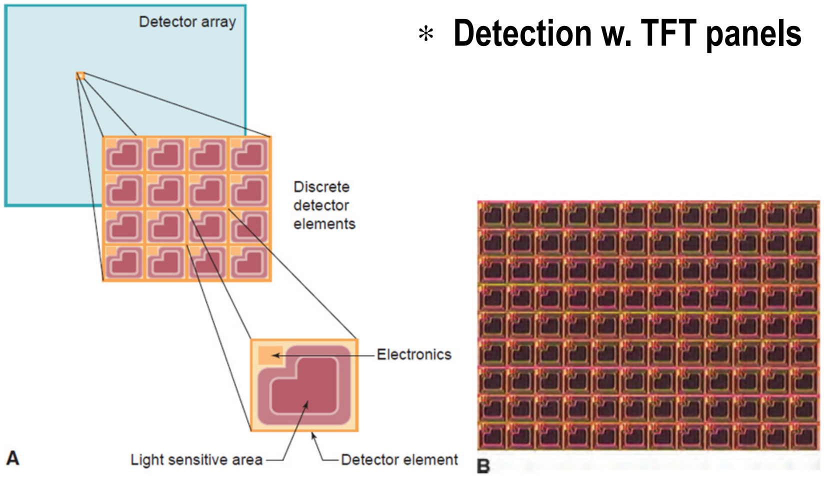

■ FIGURE 7-13 **A.** flat panel detector systems are pixelated descrete detector systems. The detector array is comprised of a large number of individual detector elements (dexels). Each dexel has a light sensitive region and a light-insensitive area where the electronic components are located. **B.** A photomicrograph of an actual TFT system is shown. The electronics component can be seen in the upper left corner of each dexel (Image courtesy John Sabol and Bill Hennessy, GE Healthcare).

Basic principles: Detection of X-ray – (3)

- **Detection with TFT panels**
  - Principles of direct and indirect detection; direct detectors use semicond. material producing electron-hole pairs proportional to X-ray

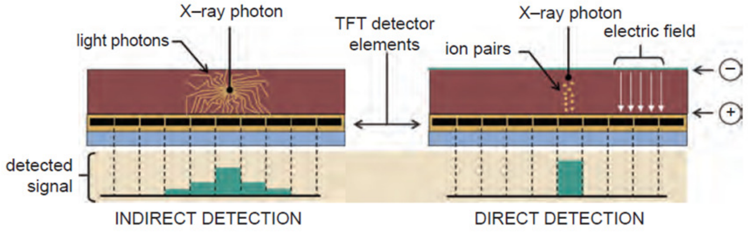

■ **FIGURE 7-15** Indirect and direct detector TFT–based x-ray detectors are shown. **A**. Photons in the indirect system propagate laterally, compromising resolution. The detected signal shown for the indirect detector shows this lateral spread in the signal from one x-ray photons interaction. **B**. For the direct detector system, the ion pairs liberated by x-ray interaction follow the electric field lines (electron holes travel upwards, electrons travel downwards) and have negligible lateral spread. Here, the detected electronic signal from one x-ray photons interaction is collected almost entirely in one detector element, and therefore better spatial resolution is achieved.

Basic principles: Detection of X-ray – (4)

- **Standard Setup with TFT panels**
  - Light bulb in collimator allows focus positioning on patient
  - Anti-scatter grid photocell improves travelling of X-ray beam process

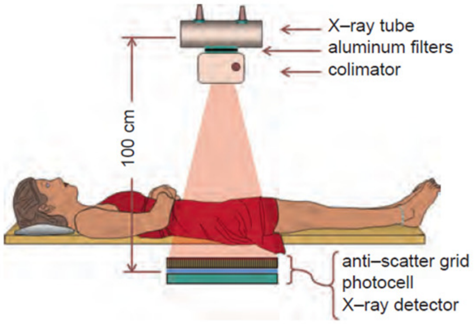

■ **FIGURE 7-16** The standard configuration for radiography is illustrated. Most table-based radiographic systems use a SID of 100 cm. The x-ray collimator has a light bulb and mirror assembly in it, and (when activated) this casts a light beam onto the patient that allows the technologist to position the x-ray beam relative to the patient's anatomy. The light beam is congruent with the x-ray beam. The x-rays that pass through the patient must pass through the antiscatter grid and the photocell (part of the AEC system) to then strike the x-ray detector.

Reference book

The Essential
Physics of
Medical Imaging

THIRD
EDITION

JERROLD T. BUSHBERG, PhD
Clinical Professor of Radiology and Radiation Oncology
University of California, Davis
Sacramento, California

J. ANTHONY SEIBERT, PhD
Professor of Radiology
University of California, Davis
Sacramento, California

EDWIN M. LEIDHOLDT JR, PhD
Clinical Associate Professor of Radiology
University of California, Davis
Sacramento, California

JOHN M. BOONE, PhD
Professor of Radiology and Biomedical Engineering
University of California, Davis
Sacramento, California

Wolters Kluwer | Lippincott Williams & Wilkins
Health
Philadelphia • Baltimore • New York • London
Buenos Aires • Hong Kong • Sydney • Tokyo

Overview Module 07 Part 1 X-ray

- **Part 1a: Basic principles of X-ray**
  - EM radiation
  - X-ray tube and detection
- **Part 1b: Clinical techniques and applications**
  - Fused visualization
  - Registration in various types: rigid, elastic, vascular
  - Clinical applications:
    - (1) Needle registration and navigation during live interventions, and
    - (2) Stenting with live artery overlay visualization

Fused visualization – (1)

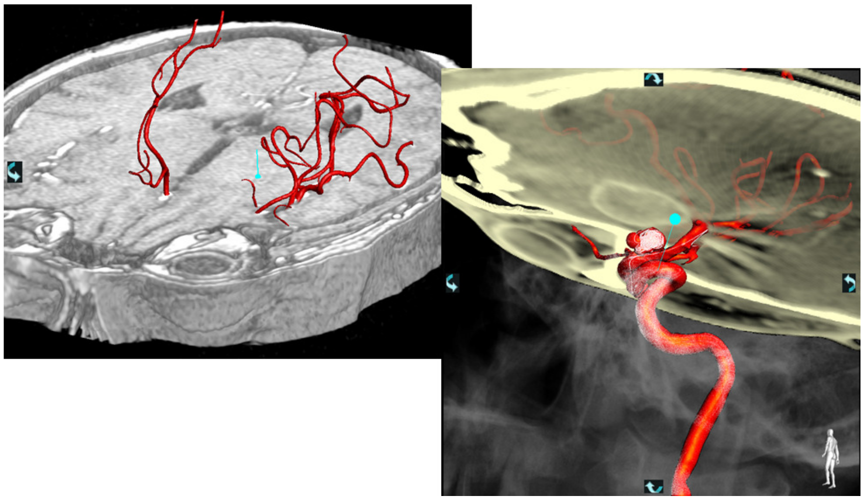

Fused Vis. – (2) / First render mesh

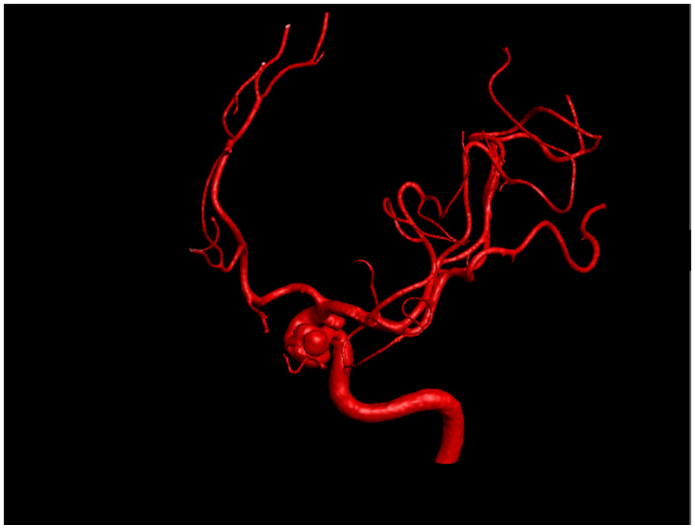

Fused Vis. – (3)

Then draw a slab of the morphological dataset

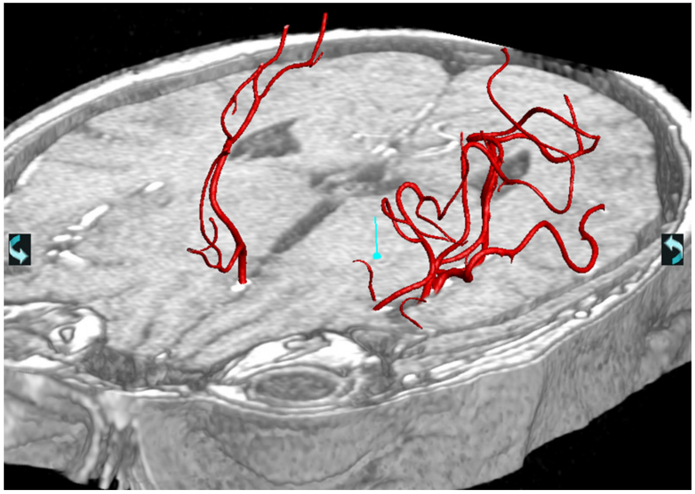

Ruijters et al.: “Silhouette Fusion of Vascular and Anatomical Data,” Proc. ISBI'06, pp. 121-124

Stencil buffer (extract vessel model)

Stencil buffer is working memory to create and work on detailed model

Click 2x

Then create fused visualization

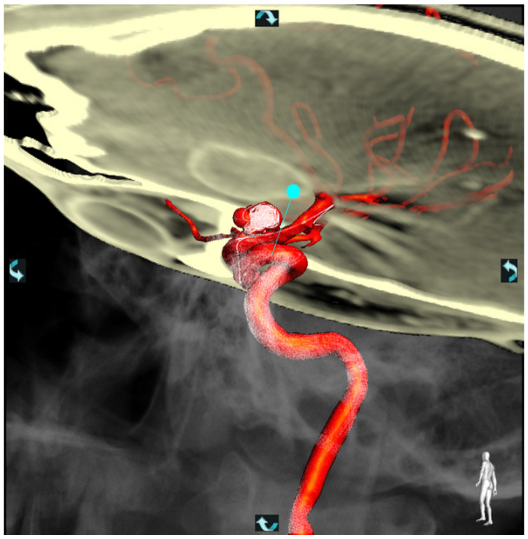

Click 3x
a. Original X-ray
b. Vessel fusion
c. Fused model visualization

Ruijters et al.:

"Real-time integration of 3-D multimodality data in interventional neuroangiography",

J. Electronic Imaging 18(3), 2009

Registration - (1) / Joint histogram

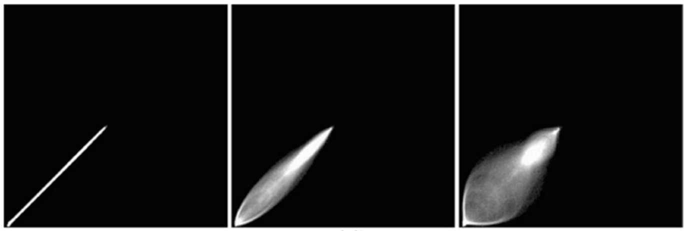

(a)

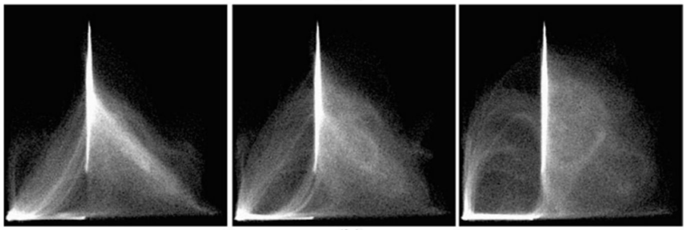

(b)

Registration – (2) / Resampling

Data of second signal needs to be re-sampled to align with sampling grid of primary signal.

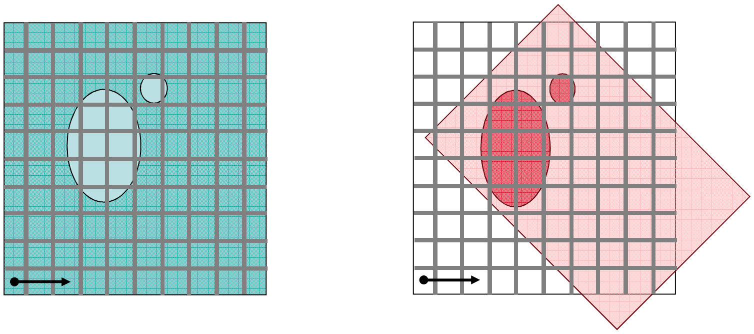

Joint histogram: increment(g,g)

Registration – (3) / 3DRA – MR, before & after

D. Ruijters: "Multi-modal image fusion during minimally invasive treatment", PhD thes. TU/e & KU Leuv., 201

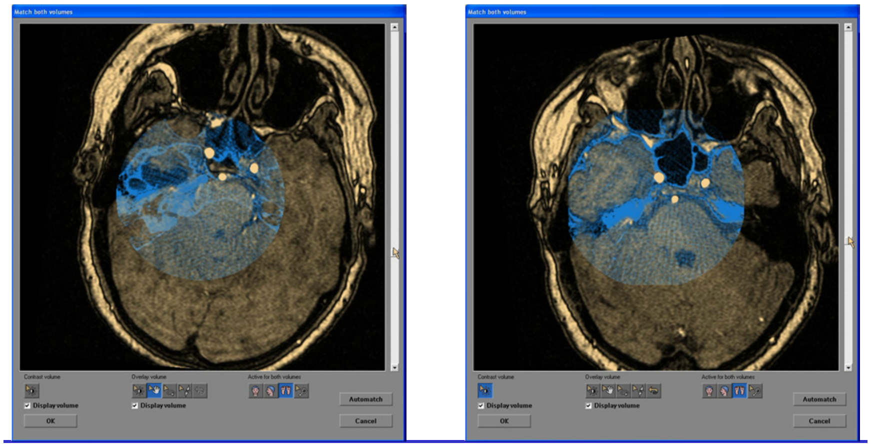

Registration – (4) / 3DRA – MR registrat.

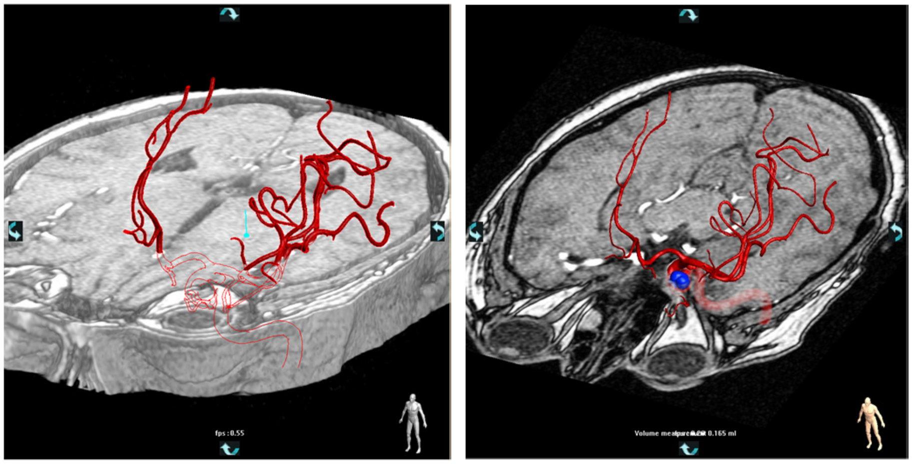

Registration – (5) /
AVM case: fused visualization

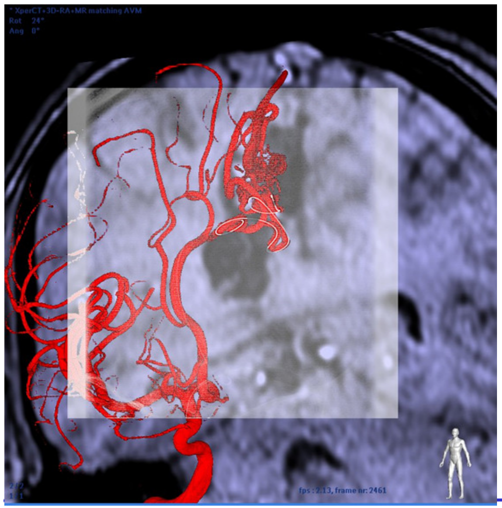

Click 3x

Ruijters et al.:
"Validation of 3D multimodality roadmapping in interventional neuroradiology",
Physics in Medicine and Biology 56(16): 5335-5354, 2011

Registration / Elastic deformation

- **Parameterized deformation:**

$$\mathbf{g}(\mathbf{x}) = \mathbf{x} + \sum_{\mathbf{j}\in J} \mathbf{c}_{\mathbf{j}} \varphi_{\mathbf{j}}(\mathbf{x})$$

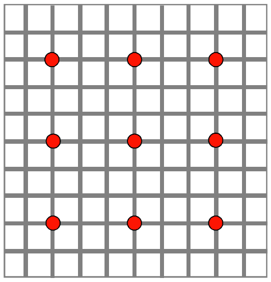

- **B-spline deformation:**

$$\mathbf{g}(\mathbf{x}) = \mathbf{x} + \sum_{\mathbf{j}\in I_c\subset\mathbb{Z}^N} \mathbf{c}_{\mathbf{j}} \beta_{n_m}(\mathbf{x}/\mathbf{h} - \mathbf{j})$$

J. Kybic, M. Unser: “Fast Parametric Elastic Image Registration”

Registration – elastic / Cubic B-spline

Sigg and Hadwiger: “Fast Third-Order Texture Filtering”, GPU Gems 2

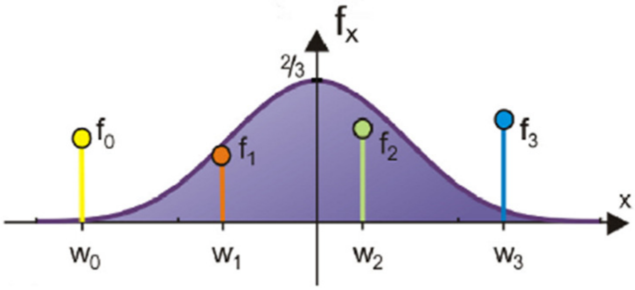

$$w_0(x)\cdot f_{i-1} + w_1(x)\cdot f_i + w_2(x)\cdot f_{i+1} + w_3(x)\cdot f_{i+2}$$

$$a\cdot f_i + b\cdot f_{i+1} = (a+b)\cdot f_{i+b/(a+b)}$$

Registration – elastic / GPU Cubic Interpolation

Real-time implementation via look-up tables

- 2D: 4 linear-interpolated lookups, instead of 16 direct lookups
- 3D: 8 linear-interpolated lookups, instead of 64 direct lookups

---

GPU Elastic Registration Iteration

1. Generate deformed image on GPU & store to texture
2. Calculate Similarity Measure & First-Order Derivative on GPU

$$\frac{\partial E}{\partial c_{\mathbf{j},m}} = \frac{1}{\|I\|} \sum_{\mathbf{i}\in I_b} \frac{\partial e_{\mathbf{i}}}{\partial f_w(\mathbf{i})} \left.\frac{\partial f_t^c(\mathbf{x})}{\partial x_m}\right|_{\mathbf{x}=\mathbf{g}(\mathbf{i})} \frac{\partial g_m(\mathbf{i})}{\partial c_{\mathbf{j},m}}$$

3. GPU is 10x faster than SSE and 100x faster than CPU

Ruijters, ter Haar Romeny, Suetens:
“Efficient GPU-Accelerated Elastic Image Registration,” Proc. BioMed 2008, pp. 419-424

Vascular Reg / 2D-3D Vessel Registration

- Intensity-based methods ☹ - landmarks too small
- Iterative Closest Point ☹ - segmentation not robust
- Conclusion: new method needed

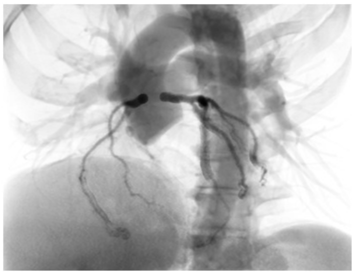

DRR

X-ray

Vascular Reg. / Vesselness Filter

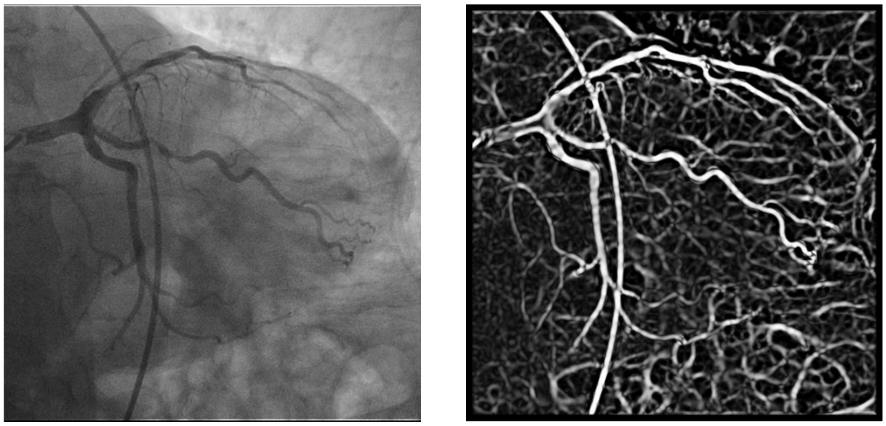

Frangi *et al.*: “Multiscale vessel enhancement filtering,” MICCAI'98, 130-137

Vascular Reg. / Distance Transform

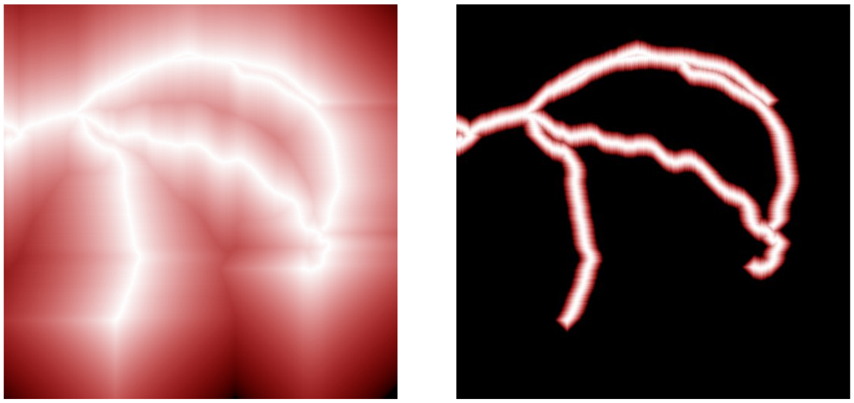

$$DT(\boldsymbol{i}) = \min_{\boldsymbol{q}\in\Omega} \|\boldsymbol{q} - \boldsymbol{i}\|$$

$$\mathcal{D}(\boldsymbol{i}) = \max\left(0,\, c - DT(\boldsymbol{i})^2\right)$$

Vascular Reg. / Similarity Measure

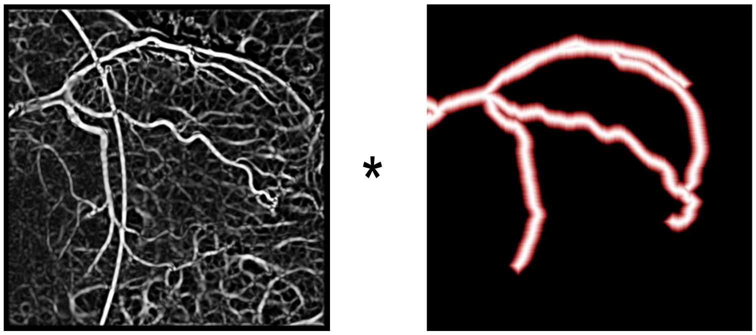

The obtained model can be registered on later X-ray images

Ruijters, ter Haar Romeny, Suetens:
“Vesselness-based 2D-3D registration of the coronary arteries",
Int. J.CARS 4:391-397, 2009

Clinical Applications – (1)
Needle-based intervention / planning

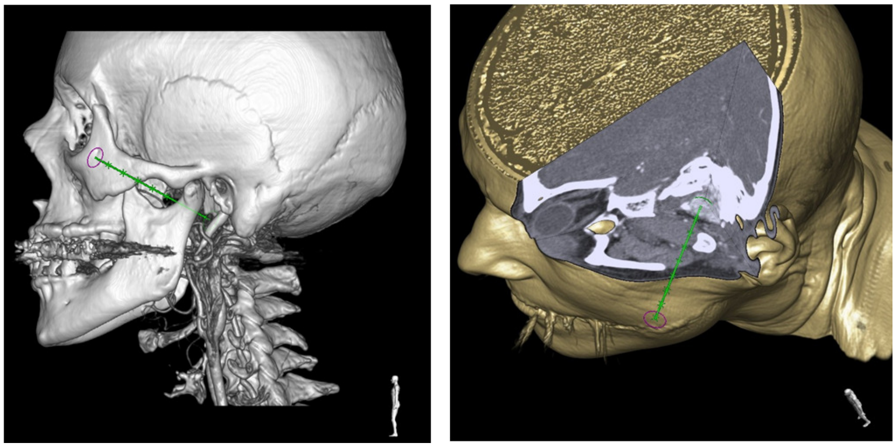

Clinical Applications – (2)
Intra-operative needle registration

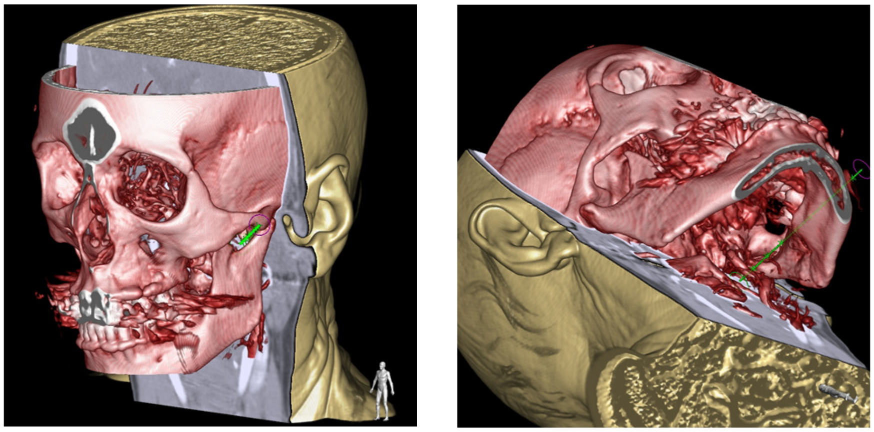

Clinical Applications – (3) Needle Navigation

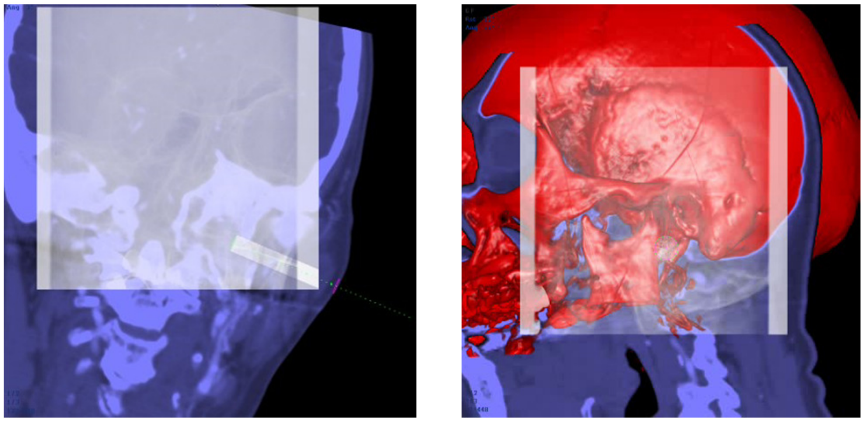

Ruijters, Spelle, Moret, Babic, Homan, Mielekamp, ter Haar Romeny, Suetens: "XperGuide: C-arm Needle Guidance", ECR 2008, Eur. Radiol. 18, Suppl 1, p. 459

Clinical Applications – (4) / Stenting for de-blocking artery

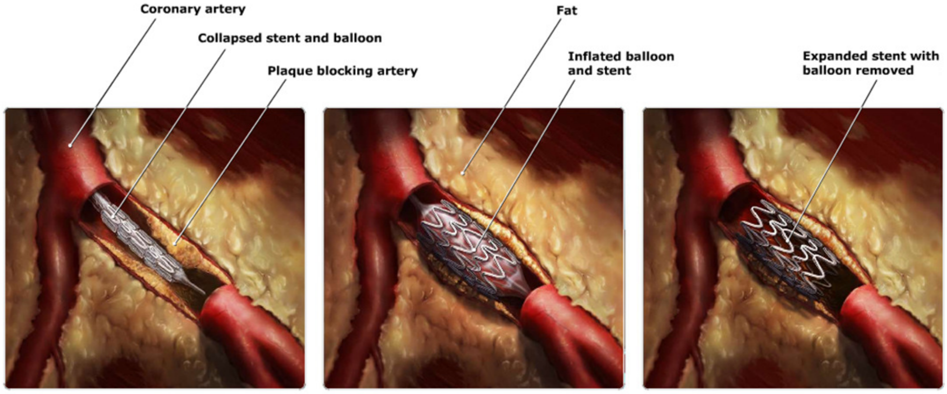

Balloon angioplasty with stent

Clinical Applications – (5)
Stenting: Overlay visualiz.

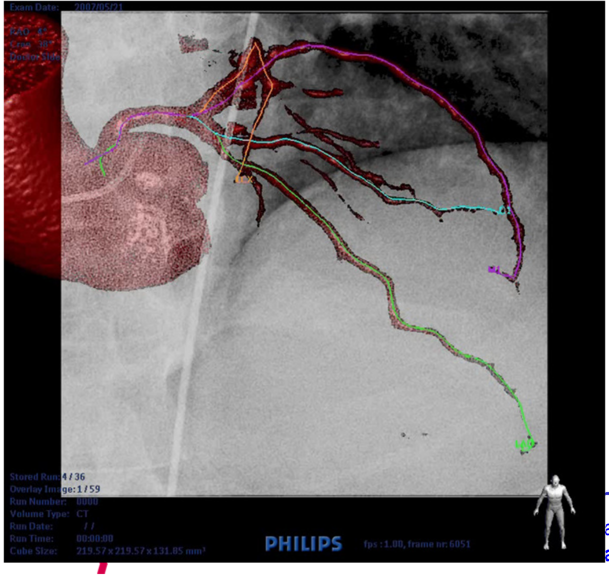

Ruijters, ter Haar Romeny, Suetens:

"Vesselness-based 2D-3D registration of the coronary arteries",

IJ Comp Ass Rad Surg 4(4): 391-397

Thanks to Dr. Danny Ruijters of Philips Healthcare for beautiful visual material!

Appendix slides – (1)
First-Order Derivative of Sim. Measure

$$\frac{\partial E}{\partial c_{\mathbf{j},m}} = \frac{1}{\|I\|} \sum_{\mathbf{i} \in I_b} \frac{\partial e_{\mathbf{i}}}{\partial f_w(\mathbf{i})} \left. \frac{\partial f_t^c(\mathbf{x})}{\partial x_m} \right|_{\mathbf{x}=\mathbf{g}(\mathbf{i})} \frac{\partial g_m(\mathbf{i})}{\partial c_{\mathbf{j},m}}$$

Appendix slides – (2)
Derivative of the Similarity Measure

$$\frac{\partial e_{\mathbf{i}}}{\partial f_w(\mathbf{i})}$$

SSD:
$$E = \frac{1}{\|I\|} \sum_{\mathbf{i} \in I} e_{\mathbf{i}}^2 = \frac{1}{\|I\|} \sum_{\mathbf{i} \in I} \left(f_w(\mathbf{i}) - f_r(\mathbf{i})\right)^2$$
$$= \frac{1}{\|I\|} \sum_{\mathbf{i} \in I} \left(f_t^c(\mathbf{g}(\mathbf{i})) - f_r(\mathbf{i})\right)^2$$

$$\frac{\partial e_{\mathbf{i}}}{\partial f_w(\mathbf{i})} = 2\left(f_w(\mathbf{i}) - f_r(\mathbf{i})\right)$$

Appendix slides – (3)
Derivative of the Deformed Image

$$\left.\frac{\partial f_t^c(\mathbf{x})}{\partial x_m}\right|_{\mathbf{x}=\mathbf{g}(\mathbf{i})}$$

- Sobel operator to calculate H &V gradients:

-1	0	1
-4	0	4
-1	0	1

1	4	1
0	0	0
-1	-4	-1

Appendix slides – (4)
Derivative of the Control Points

$$\frac{\partial g_m(\mathbf{i})}{\partial c_{\mathbf{j},m}}$$

$$\mathbf{g}(\mathbf{x}) = \mathbf{x} + \sum_{\mathbf{j}\in I_c\subset\mathbb{Z}^N} \mathbf{c}_{\mathbf{j}}\beta_{n_m}\left(\mathbf{x}/\mathbf{h}-\mathbf{j}\right)$$

$$\frac{\partial g_m}{\partial c_{\mathbf{j},m}} = \beta_{n_m}\left(\mathbf{x}/\mathbf{h}-\mathbf{j}\right)$$

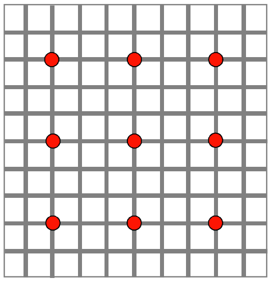

- Constant
- B-spline: separable kernel of fixed size

Appendix slides – (5)
Optimization

- Many parameters: huge parameter space
- Solution: use derivatives like Jacobian, Hessian to find direction in huge space
- Example algorithms using this principle:
  - **Gradient Descent**
  - Quasi-Newton
  - **Levenberg-Marquardt**